Chinese Chemical Letters 32 (2021) 2939–2946

Contents lists available at ScienceDirect

Chinese Chemical Letters

journal homepage: www.elsevier.com/locate/cclet

Review

Role of biochar surface characteristics in the adsorption of aromatic compounds: Pore structure and functional groups

Xue-Fei Tan[a,b], Shi-Shu Zhu[c,d], Ru-Peng Wang[b], Yi-Di Chen[b,e], Pau-Loke Show[f], Feng-Fa Zhang[a], Shih-Hsin Ho[b,*]

[a] College of Materials and Chemical Engineering, Heilongjiang Institute of Technology, Harbin 150050, China
[b] State Key Laboratory of Urban Water Resource and Environment, School of Environment, Harbin Institute of Technology, Harbin 150090, China
[c] School of Environmental Science and Engineering, Sun Yat-sen University, Guangzhou 510275, China
[d] Guangdong Provincial Key Laboratory of Environmental Pollution Control and Remediation Technology, Sun Yat-sen University, Guangzhou 510275, China
[e] State Key Laboratory of Urban Water Resource and Environment, School of Civil and Environmental Engineering, Harbin Institute of Technology (Shenzhen), Shenzhen 518055, China
[f] Department of Chemical and Environmental Engineering, Faculty of Science and Engineering, University of Nottingham Malaysia, 43500 Semenyih, Selangor, Malaysia

ARTICLE INFO

Article history:
Received 21 December 2020
Revised 17 March 2021
Accepted 30 April 2021
Available online 14 May 2021

Keywords:
Biochar
Surface characteristics
Aromatics
Adsorption
Surface functional groups

ABSTRACT

Biochar (BC) are widely used as highly efficient adsorbents to alleviate aromatics-based contaminants due to their ease of preparation, wide availability, and high sustainability. The surface properties of BCs usually vary greatly due to their complex chemical constituents and different preparation processes and are reflected in the values of parameters such as the specific surface area (SSA), pore volume/size, and surface functional groups (SFGs). The effects of SSA and pore volume/size on the adsorption of aromatics have been widely reported. However, the corresponding mechanisms of BC SFGs towards aromatics adsorption remains unclear as the compositions of the SFGs are usually complex and hard to determine. To address in this gap in the literature, this review introduces a new perspective on the adsorption mechanisms of aromatics. Through collecting previously-reported results, the parameters log*P* (logarithm of the K_{ow}), polar surface area, and the positive/negative charges were carefully calculated using ChemDraw 3D, which allowed the hydrophobicity/hydrophilicity properties, electron donor-acceptor interactions, H-bonding, and electrostatic interactions between SFGs and aromatics-based contaminates to be inferred intuitively. These predictions were consistent with the reported results and showed that tailor-made BCs can be designed according to the molecular weights, chemical structures, and polarities of the target aromatics. Overall, this review provides new insight into predicting the physicochemical properties of BCs through revealing the relationship between SFGs and adsorbates, which may provide useful guidance for the preparing of highly-efficient, functional BCs for the adsorption of aromatics.

1. Introduction

With the increasing development of industry, large amounts of aromatics are discharged into ecological surroundings as a result of environmental migration and transformation, and exhibit high toxicity towards both humans and animals [1,2]. Thus, the deployment of highly-efficient technology to eliminate aromatics present in the environment is an urgent need. Over the decades, adsorption has been regarded as the preferred method for removing organic contaminants in wastewater or groundwater [3], and various benchmark carbonaceous adsorbents such as activated carbon (AC) [4], carbon nanotubes (CNT) [5], graphene oxides (GO) [6], and biochar (BC) [7,8] have been widely used with satisfactory removal ability. Of these, BC in particular has been identified as a promising candidate for alleviating aromatics-based contaminates, owing to its relative ease of preparation, wide availability, and functional structure [9,10]. Recent studies have identified many aromatics, which, along with their derivatives, can be rapidly adsorbed by BC, such as polycyclic aromatic hydrocarbons (PAHs), chlorinated pesticide, antibiotics, and polychlorinated biphenyl [11,12]. However, as the adsorption mechanisms of aromatics on BC are still unclear, the production of tailor-made BCs designed to target specific aromatics is currently lacking, which hinders its development as a highly efficient adsorbent.

* Corresponding author.
E-mail addresses: stephen6949@hit.edu.cn, stephen6949@msn.com (S.-H. Ho).

https://doi.org/10.1016/j.cclet.2021.04.059
1001-8417/

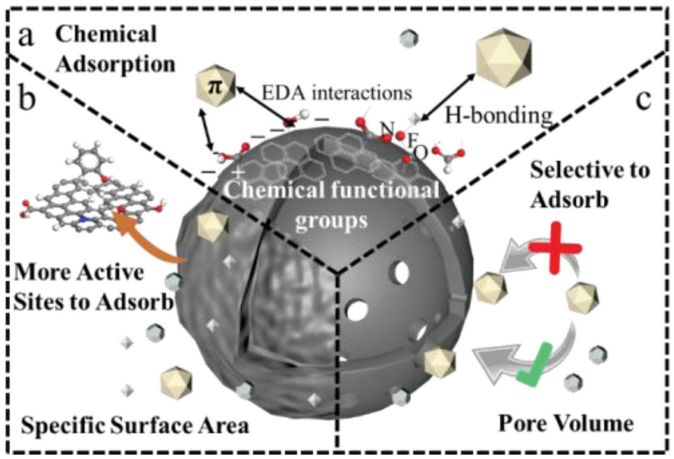

Fig. 1. (a-c) The adsorption mechanisms between biochar and aromatic compounds.

Typically, the surface structural properties of BCs, such as surface functional groups (SFGs), specific surface area (SSA), and pore volume/size, are mainly responsible for the adsorption of aromatics from the aqueous phase, as opposed to the molecular weights, chemical structures, and polarities of the target aromatics [13]. In particular, for BCs with higher pyrolysis temperatures, surface adsorption usually emerges as the dominant domain rather than the partitioning of matrix diffusion [14]. Unlike in diffusion-limiting adsorption, the surface properties of BCs regulate the interfacial bonding by means of covalent bonding, hydrogen (H–) bonding, or electron donor-acceptor (EDA) interactions [15,16]. Moreover, the pyrolysis temperature can alter the surface structure and phase of BCs. As the pyrolysis temperature increases from 100 °C to 800 °C, the surface pore sizes of BCs evolve from micropores to macropores, while moieties as functional groups gradually emerge on the defective edges of the BCs between 100 and 500 °C and are eliminated above 600 °C [17,18]. In addition, the types of functional groups (*e.g.*, oxygen-containing) appearing on the BC surface can directly affect its adsorptive properties [19]. Thus, gaining an in-depth understanding of these surface properties, which are key factors affecting the adsorption of aromatics on BCs, is of great significance.

The impact of the nature and characteristics of BC surfaces have been widely investigated through exploring the collinear relationship between surface properties and the adsorption of aromatics [20,21]. The underlying mechanisms of the interactions between aromatics and surface adsorption sites are summarized in Fig. 1, which suggests that the hydrophobic effect (weak hydrophobic interaction between solute and adsorbent surface), H-bonding (non-covalent specific interaction involving the aromatic π-system), and EDA interactions (between the dissociated SFGs and the carbonaceous layers of BCs with electronegative atoms) as shown in Fig. 1a, as well as coulombic forces, correspond to the surface functional groups and pore size or volume. Most studies focused on the large specific surface area of biochar, which can provide more active sites for adsorption (Fig. 1b). And the larger pore volume can only act as a channel, while the smaller pore volume will prevent molecules from entering the pore channel to reduce the probability of pollutants interacting with biochar. Only a suitable pore volume can promote the occurrence of adsorption reactions (Fig. 1c). However, to date, a comprehensive review focused on discussing and comparing the relationships between the surface properties of BCs and the adsorption of aromatics, as well as the underlying mechanisms, is still lacking. Therefore, to address this gap in the literature, the current paper aims to further enhance the applicability of BCs towards aromatics removal through critically reviewing, discussing, and comparing the relationships between the surface properties of BCs and the adsorption of aromatics. Additionally, and more importantly, the potential mechanisms by which the surface structures of BCs facilitate aromatics removal are also comprehensively revealed and summarized based on molecular computing analysis of data obtained from the literature using the chemical structure analysis tool ChemDraw 3D.

2. Specific surface area and pore volume

The porosity of BCs has been identified as a crucial factor in determining the adsorption of aromatics. It has also been found that the toluene adsorption capacity is linearly correlated to the BC specific surface area (SSA), with a correlation coefficient of 0.897 [22], suggesting that higher surface areas may provide more available sites for aromatics [23,24]. Thus, improving the SSA is regarded as a feasible strategy for further increasing aromatics adsorption on BCs. Several hole-making methods have been used as activation approaches for enlarging the SSA [25]. In particular, physical activation tend to result in microporous structures and larger SSAs. For instance, increasing the pyrolysis temperature could accelerate the development of porosity [26]. As the temperature increases, the unstable components in biomass such as starch, hemicellulose, and lignin tend to decompose into volatile compounds such as acetic acid, tar, methanol, CO_2, CO and H_2. The overflow of volatile compounds can turn on the blocked pore channels to form more porous structures and produce new active sites [26,27]. Moreover, condensation of the graphene layer distributed on the BC would occur, leading to the emergence of microcrystalline structures. The process of creating the random stacking graphite clusters also contributes to the enlargement of pore sizes and SSA [28].

In addition to physical activation, chemical activation methods have also been widely employed to increase the porosity of BCs. The co-pyrolysis of a dehydrating agent or a corrosive activator with biomass causes the carbon layer to undergo a series of crosslinking condensation reactions or carving operations to form microporous structures [29]. Li *et al.* [29] demonstrated that impregnating biomass with chemical activators could significantly develop the porosity and SSA and pore volume of BCs. Strong acids, alkalis, and salts, including H_2SO_4 [29], H_3PO_4 [30], KOH [31] and NaOH [32], have been identified as efficient hole-making activators; however, different chemical activation methods may result in different degrees of SSA and pore volume of BCs. For instance, it has been shown that KOH as an activator is beneficial for forming micropores, whereas H_3PO_4 is more favorable towards the creation of microporous or mesoporous, as shown in Table S1 (Supporting information) [31,33]. Moreover, apart from the type of species used for chemical activation, the incubation ratio and reaction period also have a significant impact on the development of SSA and pore structure as well as the on the ability of aromatics to adsorb on BCs.

It is also important to establish the relationships between the SSA and pore volume of BCs and the adsorption of aromatic contaminants. Zhu *et al.* [34] utilized $ZnCl_2$ to enlarge the pore volume of BC from 0.08 cm^3/g to 1.68 cm^3/g, thereby improving its adsorption capacity towards toluene. To demonstrate this effect, they divided the pore volumes of BC into four size ranges: 0.2–1.6 cm^3/g (Fig. 2a), 0.2–0.9 cm^3/g (Fig. 2b), 0.2–0.6 cm^3/g (Fig. 2c), 0.08 to 0.2 cm^3/g (Fig. 2d). Their analysis showed that pore volumes ranging from 0.2 cm^3/g to 0.9 cm^3/g were best correlated with adsorption capacity, clearly indicating that the development of appropriate pore volumes can enhance the adsorption of aromatics on BCs. This phenomenon may result from the intragranular diffusion between suitable pore volumes and toluene during the adsorption process through van der Waals forces. Simultaneously,

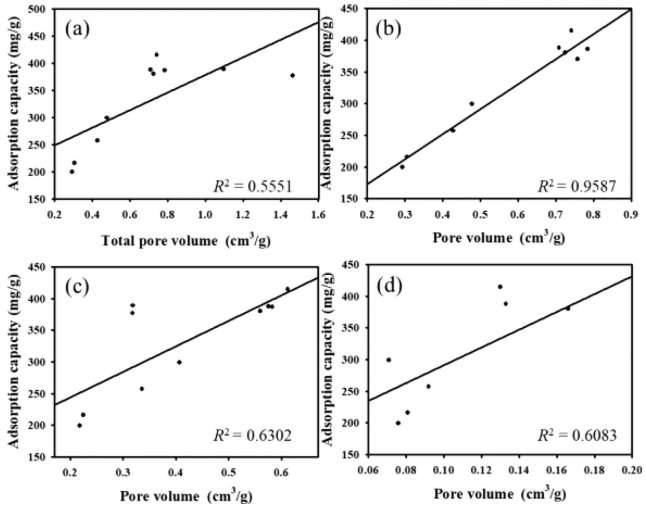

Fig. 2. The effect of pores volume on toluene adsorption. Pore volume is (a) 0.2–1.6 cm^3/g, (b) 0.2–0.9 cm^3/g, (c) 0.2–0.6 cm^3/g, (d) 0.06–0.2 cm^3/g, respectively. Modified with permission [34]. Copyright 2018, Elsevier.

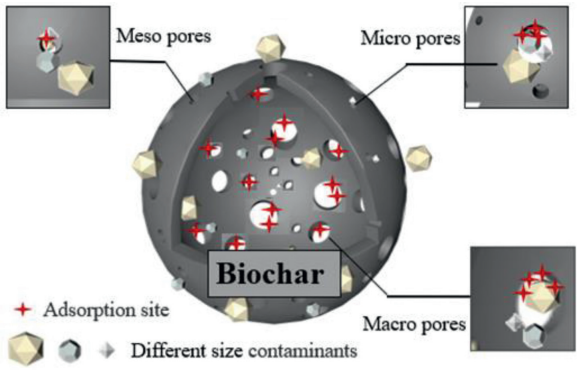

Fig. 3. The effect of pore volume/size on adsorption.

capillary condensation occurs in the mesopores, which is also an important factor affecting the adsorption efficiency [25].

Furthermore, the pore sizes of BCs also have noticeable impacts on their adsorption ability. The pores of BCs can be generally divided into macropores (> 50 nm), mesopores (2–50 nm), micropores (< 2 nm), and narrow micropores (< 1 nm) [35]. By comparison, the molecular sizes of most aromatics are much smaller than the pore sizes of most BCs, where the varied pore size leads to different adsorption mechanisms. Crespo *et al.* [36] illustrated that pore sizes of 12 and 16.8 nm on carbonaceous materials exhibited distinct adsorption capacities towards benzene and thiophene. Stronger adsorption was observed for the smaller carbonaceous. However, the presence of pore sizes far larger than the adsorbate molecular diameters would cause the interactive forces between the adsorbent and the adsorbate to be largely eliminated, resulting in the pores acting mainly as diffusion channels. Wang *et al.* [37] synthesized mesoporous carbon materials for benzene and cyclohexane adsorption, demonstrating that the diffusion coefficient of the synthesized mesoporous carbon with 5.0 nm pores was twice that of the material with 1.8 nm pores. This finding further confirms that pores which are slightly larger in size than the adsorbate can provide adsorption sites, whereas oversized pores likely enhance the diffusion of aromatics. The adsorption mechanisms of aromatics on BCs with different pore sizes are illustrated in Fig. 3.

3. Surface functional groups

It is worth noting that although the functional groups on the BC surface largely affect the chemical reactions between BCs and aromatics, it is still not straightforward to clearly identify and distinguish all of the SFGs. To date, however, several technologies, such as FT-IR, X-ray photoelectron spectroscopy (XPS), and near-edge X-ray absorption fine structure spectroscopy (NEXAFS) have been applied towards investigating these functional groups. Based on the biomass composition, and the different pretreatment, activation, and pyrolysis conditions, a given BC would possess various functional groups distributed on its surface, which greatly affect the adsorption properties.

The SFGs existing on BC are commonly classified as either oxygen-, nitrogen-, or sulfur-containing, respectively [38]. Of these, the oxygen-containing functional groups are considered the most common, and can be further divided into acidic, neutral, and basic groups based on their properties. The acidic groups normally include the carboxyl, lactonic and phenolic groups. On the other hand, the pyrone- and chromene-type groups are accepted as two common basic active sites, whose properties can be attributed to the basic nature of the carbon surface, which is more pronounced in carbon atoms without oxygen due to the presence of delocalized electrons [39]. Many studies have reported that the adsorption capacity of biochar adsorbents has increased after oxidation modification [40,41]. The introduction of nitrogen-containing functional groups can significantly enhance the polarity of the carbon surface, thereby increasing the specific interaction between pollutants and polar adsorbents [42]. Whereas, sulfur-containing functional groups can adjust the adsorption capacity of biochar by changing its specific surface area and pore volume [43,44].

During the adsorption of aromatics, and in particular ionic aromatic pollutants such as herbicides and antibiotics, various forces occur between the adsorbate and SFGs [45]. The SFGs with different physical and chemical properties interact with the adsorbent and the liquid phase depending on their typical structural characteristics. It is generally accepted that the adsorption process of the aromatics mainly depends on their chemical interactions with the multifarious SFGs of BC adsorbents [45]. The distribution, polarity, and hydrophobicity of SFGs greatly influence the adsorption capacity of aromatics *via* H-bonding, surface charges, and other interactions [45]. However, it is difficult to be intuitively observed through experiments. According to the spatial structure of SFGs, parameters such as log*P* (logarithm of the K_{ow}), PSA (polar surface area), positive and negative charges are calculated by ChemDraw 3D to measure their hydrophobicity/hydrophilicity, H-bonding, and electron donating/accepting properties, as shown in Table 1. Therefore, new insights into the relationship between SFGs and adsorbates should be provided to enable better understanding of the properties of the functional groups, paving the way for the design of "smart" surfaces with enhanced surface chemistry for achieving the goal of highly-selective adsorption of target contaminants.

3.1. Hydrophobicity/hydrophilicity of biochar

The mechanism of biochar adsorption of aromatic hydrocarbons usually depends on the surface properties of the adsorbent, the structure of the organic adsorbate and environmental conditions. Oh *et al.* [46] confirmed that the hydration of SFGs could greatly hamper the process of phenol and nitrobenzene adsorption by blocking the inherent active sites. In the case of BC, the hydrophobicity/hydrophilicity has also been used to predict the relationship between the adsorption efficiency and SFGs [47]. The polarity index (*i.e.*, the ratio (O + N)/C or O/C) is commonly recognized as an indicator of adsorbability [48], and it is often found that the hydrophobic interactions play an important role in the adsorption

Table 1
Structure, charge, log*P* and polar surface area of SFGs on biochar.

No.	Structure [b]	Atom No.	Charge	log*P* [a]	Area
1	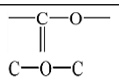	[O]	−0.14	1.82	14.10
2		[O]	−0.28	0.10	14.10
3	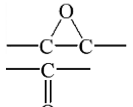	[O]	−0.41	0.48	14.10
4	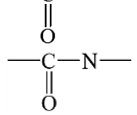	[O]	−0.53	0.03	22.30
5		[N][O]	0.23 −0.80	−0.28	35.10
6	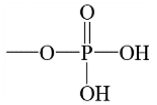	[O(2)] [P(3)] [O(4)] [O(5)] [O(6)]	−0.46 2.08 −0.50 −0.50 −1.17	0.49	84.00
7	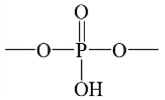	[O(2)] [P(3)] [O(4)] [O(5)] [O(6)]	−0.46 2.09 −0.46 −0.50 −1.17	0.52	74.30
8	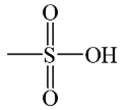	[S(2)] [O(3)] [O(4)] [O(5)]	2.63 −0.47 −1.11 −1.11	−0.99	68.40
9	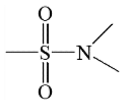	[S(2)] [N(3)] [O(4)] [O(5)]	2.59 −0.25 −1.14 −1.14	−0.87	47.30
10	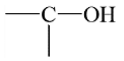	[O]	−0.35	0.35	23.80
11	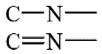	[N]	−0.23	1.71	0.00
12	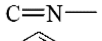	[N]	−0.14	−0.22	11.30
13	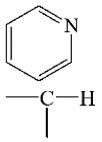	[N]	−0.21	0.35	23.80
14				1.71	0.00
15				1.48	0.00
16				1.26	0.00

[a] The log*P* parameter represents logarithm of the Kow of neutral species.
[b] The two-dimensional planar structure of surface functional groups 1–16 in Table 1 corresponds to the three-dimensional structure of surface functional groups 1–16 in Fig. 4.

of aromatics onto BC [49]. However, using the polarity index exclusively to predict the hydrophobicity/hydrophilicity of BC by the bulk elements may be inadequate, as the adsorption process usually occurs between the organic adsorbate and the adsorbent SFGs. Thus, it is necessary to determine the surface polarity, which has been employed as an alternative predictor, using XPS.

Recently, the impact of the hydrophobicity/hydrophilicity of SFGs on adsorption was also proposed as way to predict its adsorption capacity through calculating its organic solvent-water partitioning coefficient (K_{ow}) for octanol. However, although K_{ow} is related to the surface polarity of the adsorbent, it is hard to specify the polarity of each SFG on BC due to interference from surrounding factors such as ionic strength and temperature [50]. For BCs in particular, various atoms (*e.g.*, C, H, O, N, P and S) contributing to the BC structure can form different combinations of SFGs *via* the formation of hydroxyl, epoxy, carboxyl, acyl, carbonyl, ether, ester, sulfonic, pyrrole, pyridine, amine, imine, acylamide, nitroso and nitro groups on the surface [51,52]. Thus, calculating the p*Ka* (basic dissociation constants) values and concentrations of SFGs by acid-base titration is likely more effective in enabling the polarity of

the BC surface as well as its contribution towards the adsorption capacity of aromatics to be predicted [51]. Hence, in this review, we demonstrate how to predict the hydrophobicity/hydrophilicity of the BC surface by calculating the partition coefficient (log*P*) using ChemDraw 3D, based on the molecular orbital theory and the default molecular mechanics (MM2) (Table 1).

The log*P* parameter represents logarithm of the K_{ow} of neutral species [21]. Since the presence of SFGs on BC would modulate the adsorption mechanisms of aromatics due to the varied hydrophobicity, using log*P* could enable prediction of the corresponding adsorption variability information. Log*P* is driven by the free energy of the transfer from aqueous phase to nonpolar phase of the aromatics [21,53]. In this vein, several well-established mathematical correlations between chemical structure and log*P* have been developed [54,55]; however, there is barely any literature to date on the relationship between log*P* and the adsorption of aromatics on BC. According to previously-reported results [51], the common SFGs on the BC surface are shown in Table 1. The authors of the current paper hypothesized that the SFGs with different properties and pK_a values would significantly impact the log*P* values of the BC surface. The largest differences in log*P* were seen in the oxygen-containing groups with varied carbon configurations and spatial distributions, such as structures 1, 2, 3, 4 and 10 in Table 1. The merging of nitrogen and sulfur atoms with oxygen-containing groups caused the hydrophilicity of the BC to increase, with resulting log*P* values of −0.28, −0.99 and −0.87 for the nitrogen and sulfur-containing structures 5, 8, and 9, respectively, and 0.49 and 0.52 for the phosphorus-containing structures 6 and 7, respectively. As a result, using log*P* as an indicator of hydrophobicity/hydrophilicity to reliably predict the adsorption of aromatics on BC seems a promising approach, and bears further investigation.

3.2. Electron donor-acceptor interactions

Electron donor-acceptor (EDA) interactions are recognized as an important type of noncovalent specific interaction involving the aromatic π-system. Due to the graphene units often co-existing with carbonaceous adsorbents, π-EDA interactions on BC are likely to occur in the presence of ionic aromatic adsorbates [50]. Generally, the hydroxyl groups on the surface of carbonaceous adsorbents can act as electron donors, while the carboxyl functional group may act as acceptors [56].

Xie *et al.* demonstrated that π-π EDA interactions occurred between sulfamethoxazole and the aromaticity of BCs [57]. A structural analysis of the sulfamethoxazole showed that it contains an amino functional group, an N-heteroaromatic ring, and an unprotonated sulfonamide group with high electron withdrawing ability, all of which can act as strong π-electron acceptors [58]. Moreover, it has been demonstrated that π-π EDA interaction acted as an important role between a series of heteraromatic amines and graphite was also reported [47,57].

In addition, the π-π and n-π EDA interactions of anion contaminants may be increased due to the dissociation of −OH groups which are stronger electron donors compared to neutral species [59]. For instance, Wu *et al.* [60] found that the removal efficiency of naphthol using carbon nanotubes (CNTs) and graphite as adsorbents was improved, with enhanced EDA interactions, at higher pH values. In general, compared to cations and zwitterions, the adsorption capacities of anions on carbonaceous adsorbents are lower, while their π-π and n-π EDA interaction intensities are also relatively weak. Additionally, the negative repulsions occurring between the adsorbate and adsorbent due to acid groups [50]. Many aromatic amines are positively charged in a specific pH range, enabling the charges of cations located on the aromatic ring to interact with the electron-rich carbonaceous material *via* π^+-π EDA interactions [61]. Recently, ten aromatic cations (including triazine herbicides, heterocyclic aromatic amines, substituted anilines, and other amines) were reacted with pyrogenic carbonaceous materials (graphite and BCs), which clarified the function of the π^+-π EDA interactions, thus confirming that the π-electron acceptors provided by the quinoline cations could interact with graphite [62]. Further, based on the density function theory (DFT), electrons can be transferred to the ring system during adsorption, which may contribute to the enhancement of cation-π interactions [62].

On the other hand, the presence of zwitterions in amphoteric pollutants may make it difficult to obtain a detailed understanding of the different types of EDA interactions occurring and their interplay during the adsorption process. For instance, both π-π and cation-π EDA interactions may occur between tetracycline and the graphene surface [63]. It has been suggested that the varied EDA interactions play different roles between the carbonaceous adsorbents and the SFGs of amphoteric compounds (*e.g.*, quinolone groups in antibiotics) [56,64].

SFGs as the electron donor/acceptor part greatly affect the electrochemical behavior of the material, the charges of the SFGs were calculated and are shown in Fig. 4 and Table 1. By comparison, the corresponding oxygen-, phosphorous-, sulfur- and nitrogen-containing functional groups possess obvious charge characteristics. For instance, the charges of O(2) in structure 2, O(5) in structure 3, and O(4) in structure 4 (Fig. 4) are −0.288, −0.414, −0.531, respectively, resulting in their negative charges enhancing the donor strength of the electrons in the oxygen-containing functional groups. Klüpfel *et al.* also confirmed that the phenolic −OH and −C−O groups can be considered as potential electron donating capacity groups [65]. However, carboxyl −COOH, phenolic −OH and electron-rich ketones groups (−C−O), generally can be used as an electron donating group [66,67]. The establishment of N-containing and S-containing functional groups can increase the electroactive sites of BC, which is an effective method to promote the adsorption reaction. As we all know, N atoms are rich in electrons, which can adjust the electronic properties of BC and help improve the conductivity of the carbon matrix [68,69]. Because of this, the introduction of nitrogen-containing functional groups cannot only increase the adsorption rate of BC, but also increase the adsorption capacity of aromatic compounds, especially pyridine N, pyrrole N and graphite N [70]. Additionally, as the nitrogen atoms can serve as both electronic donors and receptors, the charge of N(3) in structure 5 is 0.236 (*i.e.*, positive) while other N atoms have negative charges, which suggests that N atoms located at different sites in nitrogenous functional groups play different roles in the adsorption process. Moreover, due to sulfur atoms exhibiting similar electronic receptor properties to phosphorus, positive charges were observed in structures 7, 8 and 9. Furthermore, Du et al. found that the introduction of S-containing functional groups can accelerate the reaction [71]. It has been reported that sulfur-containing functional groups, especially thiophene-S, can help induce adjacent C sites to have a higher positive charge density [72–74]. Thus, these results clearly demonstrate that the atom distribution and structure of SFGs can greatly affect the electron donating/accepting properties of carbonaceous adsorbents.

3.3. Hydrogen bonding

Another mechanism by which SFGs may have a significant impact on the adsorption of aromatics is *via* H-bonding between the dissociated SFGs and the carbonaceous layers of BCs with electronegative atoms (*e.g.*, F, N, O) in organic compounds [75,76]. These H-bonds could largely contribute to the adsorption of polar aromatics (*e.g.*, phenol and bisphenol), despite the existence of columbic forces with electrostatic repulsion [77]. However, although H-bonds have been found to occur between on series of

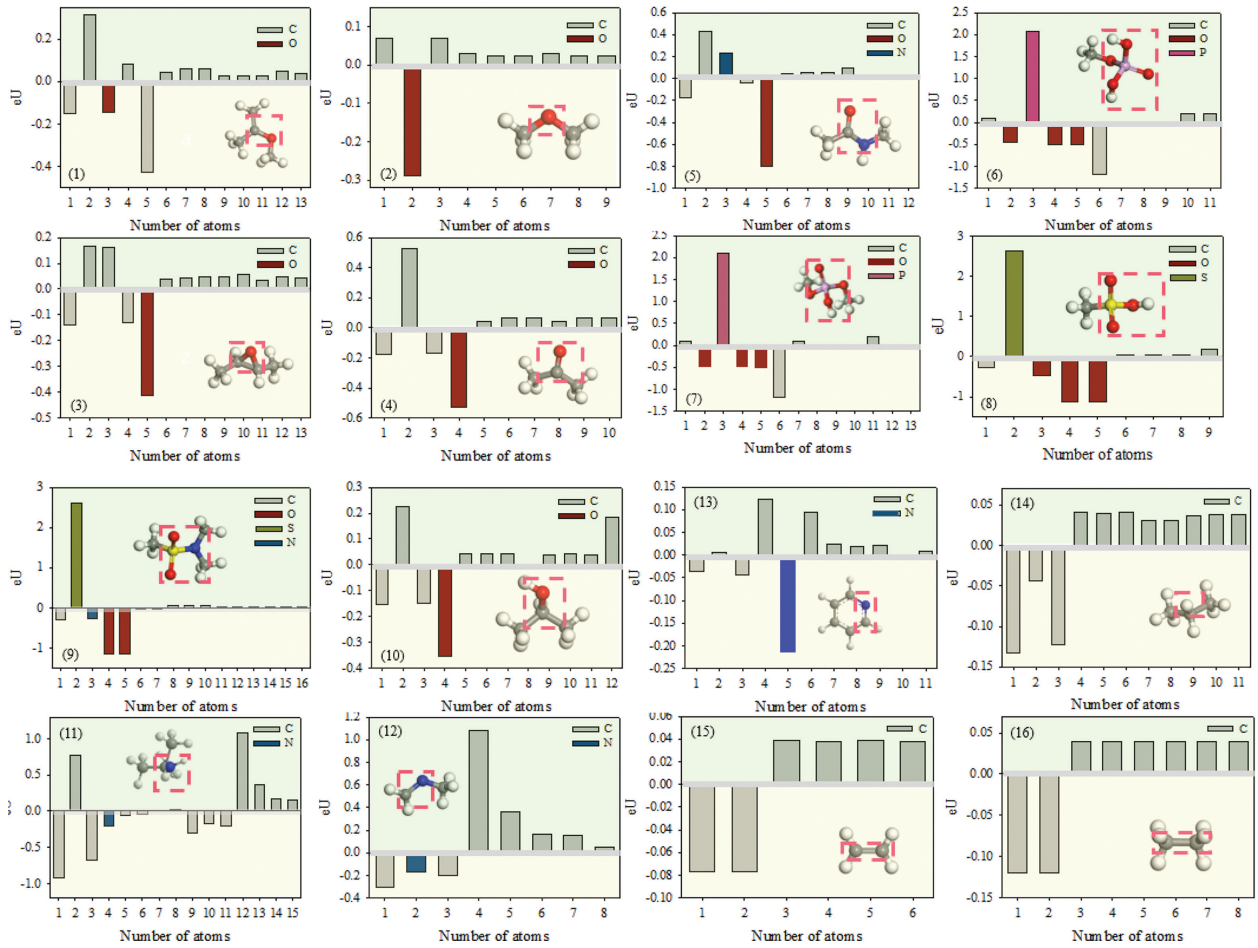

Fig. 4. The charge data of common SFGs on biochar.

adsorbents [49], intuitive evidence for the corresponding mechanism still remains elusive.

It has been reported that the polar surface area (PSA), simply defined as that part of a molecular surface corresponding to oxygen and nitrogen atoms (including the attached hydrogens), can be used as an index for measuring the H-bonding capacity [78]. Another study also demonstrated a high correlation between PSA and the numbers of H-bond donors and acceptors [79]. Thus, PSA has been applied as a useful indicator to describe the accessible area for H-bonding, and is positively correlated with the water solubility of the species as well [80]. Table 1 shows that the oxygen-containing functional groups which also contain phosphorus and sulfur (6, 7, 8, 9 in Fig. 4) have a larger PSA, which suggests that such groups could provide more H-bonding interactions between the carbonaceous adsorbent surface and aromatics. In contrast, the basic groups containing C–C and C=C on the surface of carbon material are unable to provide hydrogen bonds as their PSA is close to zero. Additionally, another type of H-bonding formed by charge strengthening (a.k.a. charge assisted hydrogen bonds –CAHBs) also largely influences the interaction properties between the ionic organic pollutants and SFGs (N, O, and S, including ester, carbonyl, nitrile, and thiol groups) during the adsorption process.

CAHBs usually have much higher bond energy than ordinary hydrogen bonds [81]. Recent studies have pointed out that (–)CAHB can be used to explain the anomalous adsorption between surface functionalized adsorbents and ionic organic compounds [82,83]. The following (–)CAHB mechanism has been proposed for carboxyl groups on biochar and CNTs with increasing pH (Eq. 1) [50]:

$$RCO_2^- + H_2O + {}^-OOC- \rightarrow (RCO_2 \cdots H \cdots OOC-)^- + OH^- \quad (1)$$

When the acid constant (p*Ka*) of the adsorbent containing O or N SFGs is close to that of the adsorbate, the effect of (–)CAHB on carbon nanotubes is stronger [81].

During the adsorption of ionized sulfadimidine by BC, Lee *et al.* found that CAHBs are an alternative route to van der Waals forces and hydrophobicity for promoting adsorption [84]. It has also been reported that the anions produced by the dissociation of sulfamethoxazole can interact with weak acid groups (such as acidic oxyl and carboxyl groups) in BCs to form CAHB, and the CAHB interactions increased with increasing p*Ka* for pollutants closer to the BC surface [85]. Furthermore, under neutral and basic conditions, the (–)CAHB interactions can be strengthened to further enhance adsorption by dissociation of pollutants [84]. Additionally, as shown in Fig. 4 and Table 1, the O atom seems to display higher electronegativity than other atoms within the oxygen-containing functional groups. In structures 6, 7, 8 and 9 (Fig. 4) in particular, the electronegativity of O atoms was noticeably enhanced when P and S atoms were present, suggesting that these atoms are electropositive within oxygen-containing functional groups.

3.4. Electrostatic interaction

Electrostatic interactions require adsorbents with positive or negative charges. Anion exchange by electrostatic attraction has recently been reported as an important contributor to the adsorption of aromatics, particularly for functionalized carbonaceous materials with amino groups [86]. In the data analysis presented in this pa-

per, it was found that the N atoms at different sites of the nitrogenous functional groups usually owned negative charges (with only structure 5 in Fig. 4 showing a positive charge), demonstrating that most of the nitrogen-containing groups would be unlikely to promote electrostatic attraction by anion exchange. On the other hand, it was found that the P atoms in the phosphorus-oxygen groups and the S atoms in the thio-oxygen groups owned some positive charges, which were 2.08 and 2.09 in structures 6 and 7 and 2.63 and 2.59 in structures 8 and 9, respectively (Fig. 4 and Table 1). Based on these finds, it can be speculated that the phosphorus-oxygen and thio-oxygen functional groups play the dominant role in strengthening the anion exchange; however, as most carbonaceous adsorbents are rich in negative charges with plentiful acid functional groups, the function of anion exchange is limited. Thus, cation exchange is likely to contribute more electrostatic interactions than anion exchange on most of the carbonaceous adsorbents.

The carbonaceous adsorbents with various SFGs usually display a superior cation exchange capacity towards positively-charged pollutants when their pK_a > PZC (the point of zero charge). Additionally, the cation exchange may be further improved by the addition of acidic groups on the adsorbent surface. For instance, Ma *et al.* confirmed that the carbon nanotubes loaded with acidic groups can increase the cation exchange capacity and show better adsorption capacity [87]. BC is also usually recognized as an excellent adsorbent due to its abundant SFGs capable of improving the cation exchange with positively-charged pollutants [88]. Additionally, all the O atoms in the oxygen-containing functional groups can carry more negative charges (Fig. 4 and Table 1), clearly suggesting that these groups greatly contribute to the electrostatic attraction by cation exchange. Moreover, in addition to electrostatic attractions, the adsorption of pollutants also contains electrostatic repulsions. However, although few studies to date have highlighted the function of electrostatic repulsion or mentioned the positive correlation between the repulsion force and the degree of oxidation of carbonaceous material [89,90], most of the electrostatic repulsions which occur between carbonaceous materials and aromatic pollutants are negligible when compared with the electrostatic attractions.

4. Conclusions

The main conclusions derived from the literature review and data analysis presented in this paper are as follows: (1) In interactions between BC adsorbents and aromatic adsorbates, the presence of adsorbent pore sizes which are only slightly larger than the molecular diameters of the adsorbates contributes to better adsorption capacity, as much larger pore sizes would act as diffusion channels due to weaker adsorptive forces. (2) Through calculation of certain parameters (such as log*P*, PSA and positive/negative charges), the mechanisms of different kinds of SFGs in the adsorption process may be analyzed. In particular, the value of log*P* can act as a predictor of the hydrophobicity/hydrophilicity on the BC surface, while the introduction of PSA allowed the H-bonding accessible area to be positively correlated with the H-bonding capacity. (3) Based on the atomic distributions and structures of SFGs, the positive/negative charges present could also be useful indicators to reflect the electron donating/accepting properties of BC. Additionally, the amount of positive/negative charges are likely responsible for the strength of electrostatic interactions. Through using these parameters calculated in this paper, the interactions between the aromatic adsorbents and the SFGs of BCs can be intuitively revealed, thus enabling both the preparation of tailor-made BCs as well as a better understanding of the physicochemical properties of aromatics.

It is hoped that this review will bring new insight into an in-depth understanding of the roles of the main surface characteristics of BCs towards the adsorption of aromatic compounds, thereby providing new information to guide the directional design of BCs, further enhancing their adsorption efficiency.

Declaration of competing interest

The authors declare no conflict of interest.

Acknowledgment

This study was funded by the National Natural Science Foundation of China (No. 51961165104), Project of Thousand Youth Talents (No. AUGA2160100917), University Nursing Program for Young Scholars with Creative Talents in Heilongjiang Province (No. UNPYSCT-2020050) and Provincial Leading Talent Echelon Cultivation Project of Heilongjiang Institute of Technology (No. 2020LJ04).

Appendix A. Supplementary data

Supplementary material associated with this article can be found, in the online version, at doi:10.1016/j.cclet.2021.04.059.

References

[1] A.Z. Redding, S.E. Burns, R.T. Upson, et al., J. Colloid Interface. Sci. 250 (2002) 261–264.
[2] Y. Chen, Y.C. Lin, S.H. Ho, et al., Bioresour. Technol. 259 (2018) 104–110.
[3] M. Ahmaruzzaman, D.K. Sharma, Colloid Interface Sci. 287 (2005) 14–24.
[4] K.C. Bedin, A.C. Martins, A.L. Cazetta, et al., Chem. Eng. J. 286 (2016) 476–484.
[5] O.G. Apul, Q. Wang, Y. Zhou, et al., Water Res. 47 (2013) 1648–1654.
[6] M.D .F.. Hossaina, N. Akthera, Zhou Y, Chin. Chem. Lett. 31 (2020) 2525–2538.
[7] Z. Liu, D. Tian, F. Shen, et al., Chin. Chem. Lett. 30 (2019) 2221–2224.
[8] Y. Ge, S. Zhu, J.-.S. Chang, et al., Environ. Pollut. 265 (2020) 115087.
[9] Y. Chen, R. Wang, X. Duan, et al., Water Res. 187 (2020) 116390.
[10] S.H. Ho, Y. Chen, R. Li, et al., Water Res 159 (2019) 77–86.
[11] Y. Chen, F. Liu, N. Ren, et al., Chin. Chem. Lett. 31 (2020) 2591–2602.
[12] X. Wang, F. Aulenta, S. Puig, et al., Environ. Sci. Technol. 1 (2020) 100013.
[13] X. Yang, Y. Wan, Y. Zheng, et al., Chem. Eng. J. 366 (2019) 608–621.
[14] J. Mao, K. Zhang, B. Chen, Environ. Pollut. 253 (2019) 779–789.
[15] S. Chen, Q. Chaoxian, T. Wang, et al., J. Mol. Liq. 285 (2019) 62–74.
[16] H.N. Tran, T. Fatma, T.H.H. Nguyen, et al., J. Hazard. Mater. 394 (2020) 122255.
[17] D. O'Connor, P. Tianyue, L. Guanghe, et al., Sci. Total Environ. 621 (2018) 819–826.
[18] C. Zhang, S.H. Ho, W.H. Chen, et al., Appl. Energy 235 (2019) 428–441.
[19] K. Yang, L. Zhu, J. Yang, et al., Sci. Total Environ. 618 (2018) 1677–1684.
[20] H.Y. Cheng, B.H. Cheng, X.C. Shen, et al., J. Environ. Chem. Eng. 6 (2018) 4196–4205.
[21] S.W. Lv, J.M. Liu, H. Ma, et al., Microporous Mesoporous Matter 282 (2019) 179–187.
[22] L. Jian, G. Zhao, Polymers (Basel) 8 (2016) 369.
[23] X. Tan, S. Zhu, P.L. Show, et al., J. Hazard. Mater. 393 (2020) 122435.
[24] E. Sharifpour, H.Z. Khafri, M. Ghaedi, et al., Sonochem 40 (2018) 373–382.
[25] X. Li, L. Zhang, Z. Yang, et al., Sep. Purif. Technol. 235 (2020) 116213.
[26] C. Bouchelta, M.S. Medjram, O. Bertrand, et al., J. Anal. Appl. Pyrolysis 82 (2008) 70–77.
[27] P.J.M. Carrott, M.M.L.R.CarrottC. Suhas, et al., J. Anal. Appl. Pyrolysis 82 (2008) 264–271.
[28] S. Zhu, X. Huang, F. Ma, et al., Environ. Sci. Technol. 52 (2018) 8649–8658.
[29] Y. Li, X. Zhang, J. Deng, et al., Chem. Phys. Lett. 747 (2020) 137325.
[30] M. Chen, F. He, D. Hu, et al., Chem. Eng. J. 381 (2020) 122739.
[31] K. Mirosław, E. Broniek, Colloids Surf A Physicochem Eng. Asp. 529 (2017) 443–453.
[32] B. Acemioğlu, Int. J. Coal Prep. Util. 7 (2019) 1–23.
[33] Y. Nakagawa, M. Molina-Sabio, F. Rodríguez-Reinoso, Microporous Mesoporous Matter 103 (2007) 29–34.
[34] J. Zhu, Y. Li, L. Xu, et al., Ecotox. Environ. Saf. 165 (2018) 115–125.
[35] C.E. Brewer, V.J. Chuang, C.A. Masiello, et al., Biomass Bioenerg. 66 (2014) 176–185.
[36] D. Crespo, R.T. Yang, Ind. Eng. Chem. Res. 45 (2006) 5524–5530.
[37] G. Wang, B. Dou, Z. Zhang, et al., J. Environ. Sci. 30 (2015) 65–73.
[38] V.K. Gupta, O. Moradi, I. Tyagi, et al., Crit. Rev. Environ. Sci. Technol. 46 (2016) 93–118.
[39] C.H. Tessmer, R.D. Vidic, L.J. Uranowski, Environ. Sci. Technol. 31 (1997) 1872–1878.
[40] X. Lu, W.L. Yim, B.H. Suryanto, et al., J. Am. Chem. Soc. 137 (2015) 2901–2907.
[41] X. Zhang, B. Gao, J. Fang, et al., Chemosphere 218 (2019) 680–686.

[42] J. Rivera-Utrilla, M. Sánchez-Polo, V. Gómez-Serrano, et al., J. Hazardous Mater. 187 (2011) 1–23.
[43] K.A. Krishnan, T. Anirudhan, J. Hazard. Mater. 92 (2002) 161–183.
[44] A. Macıas-Garcıa, C. Valenzuela-Calahorro, Carbon N Y 42 (2004) 1755–1764.
[45] Z. Chen, X. Xiao, B. Chen, et al., Environ. Sci. Technol. 49 (2015) 309–317.
[46] S.Y. Oh, Y.D. Seo, Environ. Sci. Pollut. Res. 23 (2016) 951–961.
[47] F. Xiao, J.J. Pignatello, Water Res. 80 (2015) 179–188.
[48] N.K. Niazi, I. Bibi, et al., Environ. Pollut. 232 (2018) 31–41.
[49] H. Zheng, Z. Wang, J. Zhao, et al., Environ. Pollut. 181 (2013) 60–67.
[50] M. Kah, G. Sigmund, F. Xiao, et al., Water Res. 124 (2017) 673–692.
[51] X. Xiao, B. Chen, Z. Chen, et al., Environ. Sci. Technol. 52 (2018) 5027–5047.
[52] K. Zhang, J. Mao, B. Chen, Environ. Pollut. 254 (2019) 113017.
[53] A.J. Leo, Chem. Rev. 93 (1993) 1281–1306.
[54] T. Fujita, J. Iwasa, C. Hansch, et al., J. Am. Chem. Soc. 86 (1964) 5175–5180.
[55] J. Iwasa, T. Fujita, C. Hansch, et al., J. Med. Chem. 8 (1965) 150–153.
[56] H. Peng, B. Pan, M. Wu, et al., J. Hazard. Mater. 233 (2012) 89–96.
[57] M. Xie, W. Chen, Z. Xu, et al., Environ. Pollut. 186 (2014) 187–194.
[58] C. Hansch, A. Leo, R.W. Taft, Chem. Rev. 91 (1991) 165–195.
[59] B. Chen, D. Zhou, L. Zhu, Environ. Sci. Technol. 42 (2008) 5137–5143.
[60] W. Wu, W. Jiang, W. Zhang, et al., Environ. Sci. Technol. 47 (2013) 8373–8382.
[61] N.J. Singh, S.K. Min, D.Y. Kim, et al., J. Chem. Theory Comput. 5 (2009) 515–529.
[62] F. Xiao, J.J. Pignatello, Environ. Sci. Technol. 49 (2015) 906–914.
[63] L. Ji, W. Chen, L. Duan, et al., Environ. Sci. Technol. 43 (2009) 2322–2327.
[64] X. Zhu, Y. Liu, C. Zhou, et al., Carbon 77 (2014) 627–636.
[65] L. Klüpfel, M. Keiluweit, M. Kleber, et al., Environ. Sci. Technol. 48 (2014) 5601–5611.
[66] N. Chen, Y. Huang, X. Hou, et al., Environ. Sci. Technol. 51 (2017) 11278–11287.
[67] H. Chen, K.C. Carroll, Environ. Pollut. 215 (2016) 96–102.
[68] H. Wang, W. Guo, B. Liu, et al., Water Res. 160 (2019) 405–414.
[69] X. Li, Y. Jia, M. Zhou, et al., J. Hazard. Mater. 397 (2020) 122764.
[70] W. Ren, G. Nie, P. Zhou, et al., Environ. Sci. Technol. 54 (2020) 6438–6447.
[71] W. Du, Q. Zhang, Y. Shang, et al., Appl. Catal. B: Environ. 262 (2020) 118302.
[72] S. Wang, J. Wang, Chem. Eng. J. 385 (2020) 123933.
[73] P. Hu, H. Su, Z. Chen, et al., Environ. Sci. Technol. 51 (2017) 11288–11296.
[74] D.G. Kim, S.O. Ko, Chem. Eng. J. 399 (2020) 125377.
[75] M. Franz, H.A. Arafat, N.G. Pinto, Carbon N Y 38 (2000) 1807–1819.
[76] F. Lian, B. Sun, Z. Song, et al., Chem. Eng. J. 248 (2014) 128–134.
[77] W.J. Liu, F.X. Zeng, H. Jiang, et al., Bioresour. Technol. 102 (2011) 8247–8252.
[78] H. van de Waterbeemd, M. Kansy, Chimia Int. J. Chem. 46 (1992) 299–303.
[79] M.S. Lajiness, G.M. Maggiora, V. Shanmugasundaram, J. Med. Chem. 47 (2004) 4891–4896.
[80] M. Wu, B. Pan, D. Zhang, et al., Chemosphere 90 (2013) 782–788.
[81] X. Li, J.J. Pignatello, Y. Wang, et al., Environ. Sci. Technol. 47 (2013) 8334–8341.
[82] M.B. Ahmed, J.L. Zhou, H.H. Ngo, et al., Bioresour. Technol. 238 (2017) 306–312.
[83] P. Wang, D. Zhang, H. Tang, et al., J. Hazard. Mater. 371 (2019) 513–520.
[84] J.W. Lee, M. Kidder, B.R. Evans, et al., Environ. Sci. Technol. 44 (2010) 7970–7974.
[85] M. Teixidó, J.J. Pignatello, J.L. Beltrán, et al., Environ. Sci. Technol. 45 (2011) 10020–10027.
[86] M. Auta, B.H. Hameed, J. Ind. Eng. Chem. 20 (2014) 830–840.
[87] J. Ma, F. Yu, L. Zhou, et al., Appl. Mater. Interfaces 4 (2012) 5749–5760.
[88] M. Inyang, B. Gao, A. Zimmerman, Chem. Eng. J. 236 (2014) 39–46.
[89] C.Y. Tang, Q.S. Fu, D. Gao, et al., Water Res. 44 (2010) 2654–2662.
[90] F. Xiao, X. Zhang, P. Lee, et al., Environ. Sci. Technol. 45 (2011) 10028–10035.